Sensitized photooxidation of *ortho*-prenyl phenol: Biomimetic dihydrobenzofuran synthesis and total $^1O_2$ quenching

Shakeela Jabeen,[1,2] Goutam Ghosh,[1,2] Lloyd Lapoot,[1,3] Andrés M. Durantini,[1,2,4] and Alexander Greer[1-3]*

[1] Department of Chemistry, Brooklyn College of the City University of New York, Brooklyn, New York 11210, United States

[2] Ph.D. Program in Chemistry, The Graduate Center of the City University of New York, 365 Fifth Avenue, New York, New York 10016, United States

[3] Ph.D. Program in Biochemistry, The Graduate Center of the City University of New York, 365 Fifth Avenue, New York, New York 10016, United States

[4] IDAS-CONICET, Departamento de Química, Facultad de Ciencias Exactas, Físico-Químicas y Naturales, Universidad Nacional de Río Cuarto, Ruta Nac. 36 Km 601, X5804BYA Río Cuarto, Córdoba, Argentina

*Corresponding author e-mail: agreer@brooklyn.cuny.edu (Alexander Greer)

ABSTRACT

The sensitized photooxidation of *ortho*-prenyl phenol is described with evidence that solvent aproticity favors the formation of a dihydrobenzofuran [2-(prop-1-en-2-yl)-2,3-dihydrobenzofuran], a moiety commonly found in natural products. Benzene solvent increased the total quenching rate constant (k_T) of singlet oxygen with prenyl phenol by ~10-fold compared to methanol. A mechanism is proposed with preferential addition of singlet oxygen addition to prenyl site due to hydrogen bonding with phenol OH group, which causes a divergence away from the singlet oxygen 'ene' reaction toward the dihydrobenzofuran as the major product. The reaction is a mixed photooxidized system since an epoxide arises by a type I sensitized photooxidation.

Keywords: visible light, synthesis, photosensitization, regioselectivity, prenylated phenolics, dihydrobenzofuran

INTRODUCTION

Strategies to synthesize 2,3-dihydrobenzofuran natural products have attracted attention (1-8). One strategy was the cyclization of a prenylated phenol, (*E*)-4-(2-hydroxyphenyl)-2-methyl-2-butenyl methyl carbonate **1** to reach dihydrobenzofuran (*R*)-**2** (Figure 1) (9). Dihydrobenzofuran (*R*)-**2** is related to important biologically active natural products, including tremetone (*R*)-**3** from the herb white snakeroot (*Ageratina altissima*) (10-13), and new strategies to reach them are needed.

[Figure 1 here]

Visible-light strategies to synthesize dihydrobenzofurans include successful photoredox reactions of *ortho*-quinone methides (14) and [3 + 2] cycloadditions of phenols and styrenes (15). Visible-light strategies also include sensitized photooxidation, that upon irradiation of a sensitizer, singlet oxygen ($^1O_2$) is efficiently produced (type II reaction), as well as amounts of oxygen radicals (type I) (16-18). Reports described sensitized photooxidation which gave dihydrobenzofurans, including literature examples of (−)-adunctin E (19) and dehydroisoeugenol (20). We hypothesized that the sensitized photooxidation of *ortho*-prenyl phenol (**4**) will form a dihydrobenzofuran and that mechanistic insight will enable path manipulation to it, which is the subject of this paper.

Our work sought to elucidate mechanistic details on three fronts: whether (1) sensitized-photooxidation of prenyl phenol **4** leads to dihydrobenzofuran and allylic hydroperoxides, (2) solvent effects and competition exists between type I (oxygen radicals and ions) and type II

($^1O_2$) processes (16,17), and (3) total quenching rate constant (k_T) data of $^1O_2$ can yield new insight. The results provide evidence for the mechanism shown in Figure 2, which reveals solvent *a*proticity increasing the reactivity of $^1O_2$ with the prenyl group in **4** and thus formation of dihydrobenzofuran.

[Figure 2 here]

METHODS AND MATERIALS

General. Benzaldehyde, DABCO, 3,3-dimethylallyl bromide, *meta*-chloroperoxybenzoic acid (MCPBA, 77% purity with *m*-chlorobenzoic acid as the impurity), 2-methyl-2-pentene, NaH, $NaHCO_3$, $NaNO_2$, Na_2SO_4, and phenol were purchased from Sigma-Aldrich and used as received. Aluminum (III) phthalocyanine chloride tetrasulfonic acid ($AlPcS_4$) and tetraphenylporphyrin (TPP) were purchased from Frontier Scientific and used as received. Diethyl ether, ethyl acetate, hexanes, H_2O_2 (3 w/v%), pyridine, toluene (anhydrous), $CHCl_3$, $CDCl_3$, CH_2Cl_2, CD_3CN, C_6H_6, and C_6D_6 were purchased from VWR and used as received. Previously reported syntheses were used for prenyl phenol **4** (21) and 8-acetoxymethyl-2,6-dibromo-1,3,5,7-tetramethyl pyrromethene fluoroborate (Br_2B-OAc) (22). Epoxide **8** was synthesized in 24.0±2.2% yield by the reaction prenyl phenol **4** (1.54 mmol) with MCPBA (1.92 mmol) in 3.3 mL $CHCl_3$ at 0 °C, which was followed by washing with 10% $NaHCO_3$, drying over Na_2SO_4, solvent removal, and silica gel column chromatography with hexanes/ethyl acetate (8:2).

Photooxidation reactions. Photooxidations of prenyl phenol **4** (0.10 M) were carried out in O_2-saturated C_6D_6 with TPP (0.1 mM) and in some cases DABCO (2 or 10 mM) or CH_3OH

74 with $AlPcS_4$ (0.1 mM). Solutions were pre-saturated with O_2 and the TPP or $AlPcS_4$ sensitizers
75 irradiated with two 400-W metal halide lamps through a longpass ≥ 400-nm filter solution (1-cm
76 75 w/v% $NaNO_2$) at 26 °C. Temperature increases were ≤ 3 °C over the course of the photolysis.
77 Following photolyses carried out in CH_3OH, solvent was evaporated and replaced with $CDCl_3$
78 for NMR analysis. Benzaldehyde was unreactive under the reaction conditions and therefore
79 used as an NMR internal standard.

80 2-(3-Methyl-2-butenyl)phenol **4**. ^{1}H NMR (400 MHz, $CDCl_3$) δ 7.17 – 7.11 (2H, m),
81 6.89 (1H, td, *J* = 7.4, 1.2 Hz), 6.83 (1H, dd, *J* = 8.5, 1.2 Hz), 5.37 – 5.33 (1H, m), 5.14 (1H, s),
82 3.39 (1H, d, *J* = 7.2 Hz), 1.81 (6H, s).

83 2-(Prop-1-en-2-yl)-2,3-dihydrobenzofuran **2** is a known compound (9). ^{1}H NMR (400
84 MHz, $CDCl_3$): δ 7.14 (2H, d, *J* = 8.0 Hz), 6.91-6.87 (1H, m), 6.84-6.81 (1H, m), 5.10 (1H, t, *J* =
85 1.2 Hz), 5.02 (1H, d, *J* = 4.0 Hz), 4.97 (1H, d, *J* = 4.0 Hz), 3.35 (1H, d, *J* = 8.0 Hz), 3.27 (1H, d,
86 *J* = 8.0 Hz), 1.80 (3H, s).

87 2-(2-Hydroperoxy-3-methylbut-3-en-1-yl)phenol **6**. ^{1}H NMR (400 MHz, C_6D_6): δ 11.43
88 (1H, s), 7.01-6.96 (1H, d, *J* = 8.0 Hz), 6.83-6.79 (1H, m), 6.81 (1H, m), 6.52 (1H, d, *J* = 8.0 Hz),
89 5.01 (1H, d, *J* = 1.6 Hz,), 5.00 (1H, d, *J* = 1.6 Hz), 4.80 (1H, t, *J* = 1.6 Hz,), 3.31 (1H, d, *J* = 12
90 Hz), 3.27 (1H, d, *J* = 8.0 Hz), 1.56 (3H, s).

91 (*E*)-2-(3-Hydroperoxy-3-methylbut-1-en-1-yl)phenol **7**. ^{1}H NMR (400 MHz, C_6D_6): δ
92 9.60 (1H, s), 7.01-6.96 (1H, d, *J* = 8.0 Hz), 6.83-6.79 (1H, m), 6.81 (1H, m), 6.52 (1H, d, *J* = 8.0
93 Hz), 6.33 (2H, d, *J* = 16.0 Hz), 1.56 (3H, s), 1.52 (3H, s).

94 2-((3,3-Dimethyloxiran-2-yl)methyl)phenol **8** is a known compound (23). ^{1}H NMR (400
95 MHz, C_6D_6): δ 7.08 – 7.06 (2H, m), 7.01 – 6.96 (2H, m), 2.87 (1H, d, *J* = 8 Hz), 2.84 (1H, d, *J* =
96 8.0 Hz), 2.74 (1H, t, *J* = 8.0 Hz), 1.55 (3H, s), 1.52 (3H, s).

H_2O_2. ^1H NMR (400 MHz, C_6D_6) broad δ 9.16 ppm; ^1H NMR (400 MHz, CD_3CN) δ 9.77 ppm; ^1H NMR (400 MHz, $CDCl_3$) δ 9.57 ppm; values were consistent to those reported in literature (24,25). In C_6D_6, doping with commercial H_2O_2 and the addition of co-solvent CD_3CN to solubilize was carried out to verify the NMR signal. In CH_3OH, H_2O_2 was detected after solvent evaporation and replacement with $CDCl_3$.

Total quenching rate constant determinations. The setup (26) used 532 nm light (10 mJ/pulse) from an Nd:YAG Q-switched laser operating at 5 Hz. Br_2B-OAc (2.6 μM) was used as the sensitizer in C_6H_6 or CH_3OH solutions of prenyl phenol **4** at 26 °C. A H10330A-45 (Hamamatsu Corp.) photomultiplier tube operating at -650 V was used to detect the $^1O_2$ phosphorescence. The phosphorescence was monitored through a band-pass filter centered at 1270 nm (OD4 blocking, FWHM = 15 nm) and signals collected on a 600 MHz oscilloscope. Kinetic data were fitted with a monoexponential function shown in eq 1,

$$I = I_0 + \mathrm{A}e^{-t/\tau_\Delta} \quad (1)$$

where I is the final intensity, I_0 is the initial intensity, t is the time, A is the amplitude, and τ_Δ is the lifetime of $^1O_2$. The total quenching rate constants (k_T) were obtained by fitting the data plotted of k_{obs} vs [prenyl phenol] with eq 2,

$$k_{obs} = k_d + (k_T)[\text{prenyl phenol } \mathbf{4}] \quad (2)$$

where k_{obs} is the observed $^1O_2$ quenching rate constant, k_d is the rate constant of deactivation of $^1O_2$ by the solvent.

RESULTS AND DISCUSSION

Product formation. The sensitized photooxidation reaction of prenyl phenol **4** (taken to ≤ 30% conversion) led to products **2**, and **6**-**8** according to NMR (Table 1). Attempts were not made to isolate the 2° and 3° allylic hydroperoxides **6** and **7** due to the anticipated instability to column chromatography; the proton NMR hydroperoxy and alkene signals are similar to those reported in literature (27). The stabilities of hydroperoxides vary, on detection of **6** and **7** by NMR their decomposition was not seen in the reaction mixture over several hours. The identity of epoxide **8** was verified by its independent synthesis from **4** with MCPBA. There was evidence for the formation of H_2O_2 in the reaction, but was not quantitated as we and others (24,25) have noted a broad proton NMR signals from 9.16-9.77 ppm depending on solvent. The solvent was also found to modify the product yields.

Effect of solvent on product formation. In C_6D_6, dihydrofuran **2** was the main product, along with epoxide **8**, with only small amounts of allylic hydroperoxides **6** and **7**. In CH_3OH, the amount of the dihydrofuran **2** decreased and amounts of allylic hydroperoxides **6** and **7** increased, but the amount of epoxide **8** remained nearly constant. The ratio of dihydrofuran **2** to hydroperoxides **6** and **7** is ~9:1 in C_6D_6, and ~2:3 in CH_3OH. Thus, there is a ~4-fold decrease in dihydrofuran **2** in CH_3OH compared to C_6D_6. The ratio of hydroperoxides **6**:**7** is not found to depend on C_6D_6 and CH_3OH solvent, wherein the ratio of **6**:**7** in either solvent is ~0.9:1. In C_6D_6 and CH_3OH, the yield of epoxide **8** remained nearly constant, which led us to study the addition of the known $^1O_2$ quencher DABCO (28). The addition of DABCO in the sensitized photooxidation of prenyl phenol **4** led to an absence in the formation of **2**, **6**, and **7**, however the amount of epoxide **8** formed was not affected pointing to its formation by a type I process. The

probable type I contribution led us to measure the quenching rate constants with $^1O_2$ to directly assess the type II process.

[Table 1 here]

Effect of solvent on the total $^1O_2$ quenching rate constant. Time-resolved singlet oxygen phosphorescence quenching studies provided insight to the solvent effects. The total quenching rate constant (k_T) of $^1O_2$ by prenyl phenol **4** was measured in C_6H_6 and CH_3OH by monitoring its phosphorescence quenching at 1270 nm (Table 2). Figure 3A and 3B show the decay curves are first-order and the lifetime (τ_{obs}) diminishes with increasing concentration of prenyl phenol **4** in C_6H_6 and CH_3OH. The k_T values were obtained from the linear fit of the k_{obs} ($1/\tau_{obs}$) vs [prenyl phenol] showing a k_T value ~10-fold greater in C_6H_6 in than CH_3OH (Figure 4A and 4B). This enhancement contrasts to solvent effects in di- and trisubstituted alkenes in aprotic to protic solvents that usually vary ≤ 2-fold (29,30). This aprotic solvent enhancement provides us with implications on the reaction mechanism, as we will discuss next.

[Figures 3 and 4 here]

[Table 2 here]

Mechanism of photooxidation. The above results are rationalized in the mechanism shown in Figure 2, and as follows: An experimental result is that dihydrobenzofuran formation depends on whether benzene or methanol solvent is used. The interaction of $^1O_2$ with the prenyl phenol **4** in benzene (Figure 2, path A) and in methanol (Figure 2, path B) can account for the ~10-fold greater total quenching k_T. Data over a wider solvent range to compare not only hydrogen bonding ability, but also polarity $E_T(30)$ scales are presently not available. With the

available data, dihydrobenzofuran formation is proposed to involve H-bond interaction of phenolic hydrogen with $^1O_2$, directing it to the C^{10} site in **5**. The formation of a peroxy intermediate seems plausible, but evidence has not been found with preliminary trapping experiments using triaryl phosphites. The $^1O_2$ 'ene' regioselectivity in formation of the 2° and 3° allylic hydroperoxides **6** and **7** (ratio of ~1:1) did not depend on whether benzene or methanol was the solvent. This is consistent with the *cis-effect* rule of the reaction of $^1O_2$ with trisubstituted alkenes, in which the more alkyl substituted side of the double bond is more reactive (31). Previous reports have shown instances where H-abstraction from the *exo* methyl group in trisubstituted alkenes contribute only a minor 5-10% in the formation of the 2° allylic hydroperoxide. In the presence of DABCO, the reaction did not form **2**, **6**, and **7**, however the epoxide **8** yield was unaffected pointing to a type I process in its formation (Figure 2, path C). These studies were carried out with DABCO concentrations that were insufficient to quench the sensitizer excited states, however the results do not rule out the epoxide's formation via a peroxy prenyl phenol intermediate in a self-epoxidation process.

CONCLUSION

An interesting result of this study is the increased dihydrobenzofuran formation, when the photooxidation of **4** was carried out in aprotic solvent. This result points to adduct formation **5**, which decomposes to more stable species, **2** and H_2O_2. Decreasing the proticity of the solvent increases the interaction of $^1O_2$ with the phenolic hydrogen increasing the yield of dihydrofuran from 20.0% in benzene compared to 5.1% in methanol. The k_T value showed a ~10-fold

enhancement in benzene compared to methanol. Reported differences in product formation have been seen in *t*-propenyl anisole with solvent aproticity showing increased [2 + 4] product relative to the [2 + 2] product in protic solvent (32), although the present work shows no evidence for [2 + 2] products. The present work does show evidence for a type I process to account for the formation of epoxide **8** in both solvents. Solvent, structure, and interfacial effects are subjects of continued interest in the areas of type I and type II sensitized photooxidation in terms of synthesis and mechanistic studies (16-18,33-41).

We are currently exploring (i) heterogeneous systems aimed at amplifying the formation of dihydrobenzofurans, (ii) whether a self-trapping reaction with **4** arises by a peroxy intermediate in the **4**–$^1O_2$ reaction, and (iii) whether dihydrobenzofuran **2** reacts further by $^1O_2$ [2 + 4] cycloaddition to form endoperoxides by analogy to phenol and naphthalene-1,5-diol (juglone)–$^1O_2$ reactions to reach an endoperoxide (42).

ACKNOWLEDGMENTS: Support from the National Science Foundation (CHE-1856765 and CHE-2154133) is acknowledged. We thank Leda Lee for assistance with the graphic arts.

ORCID

Shakeela Jabeen: 0000-0002-7153-3379

Goutam Ghosh: 0000-0002-2021-4589

Lloyd Lapoot: 0000-0001-6888-2626

Andrés M. Durantini: 0000-0002-7898-4033

Alexander Greer: 0000-0003-4444-9099

206

207

REFERENCES

1. Dapkekar, A. B., C. Sreenivasulu, D. Ravi Kishore and G. Satyanarayana (2022) Recent advances towards the synthesis of dihydrobenzofurans and dihydroisobenzofurans. *Asian J. Org. Chem.* **11**, e202200012.
2. Yu, X., Q. Y. Meng, C. G. Daniliuc and A. Studer (2022) Aroyl fluorides as bifunctional reagents for dearomatizing fluoroaroylation of benzofurans. *J. Am. Chem. Soc.* **144**, 7072–7079.
3. Zhang, G., X. Pan, B. Yang, L. Li and Z. Liu (2022) The asymmetric total synthesis of (−)-Eurothiocin A and its enantiomer. *J. Nat. Prod.* **85**, 997–1005.
4. Chen, Z., M. Pitchakuntla and Y. Jia (2019) Synthetic approaches to natural products containing 2,3-dihydrobenzofuran skeleton. *Nat. Prod. Rep.* **36**, 666–690.
5. Saleeb, M., S. Mojica, A. U. Eriksson, C. D. Andersson, Å. Gylfe and M. Elofsson (2018) Natural product inspired library synthesis: Identification of 2,3-diarylbenzofuran and 2,3-dihydrobenzofuran based inhibitors of *Chlamydia trachomatis*. *Eur. J. Med. Chem.* **143**, 1077–1089.
6. Natori, Y., H. Tsutsui, N. Sato, S. Nakamura, H. Nambu, M. Shiro and S. Hashimoto (2009) Asymmetric synthesis of neolignans (−)-*epi*-conocarpan and (+)-conocarpan via Rh(II)-catalyzed C−H insertion process and revision of the absolute configuration of (−)-*epi*-conocarpan. *J. Org. Chem.* **74**, 4418–4421.
7. Wang, Y. and A. Zhang (2009) Expeditious synthesis of 2,3-dihydro-2-alkoxy-3-methylenebenzofurans from *N*-benzofuran-3-ylmethyl *N,N,N*-trialkylammonium

bromides: A new approach to access the natural product, 2-hydroxy-3-methylene-6-methyl-2, 3-dihydrobenzofuran. *Tetrahedron* **65**, 6986–6990.

8. O'Malley, S. J., K. L. Tan, A. Watzke, R. G. Bergman and J. A. Ellman (2005) Total synthesis of (+)-lithospermic acid by asymmetric intramolecular alkylation via catalytic C−H bond activation. *J. Am. Chem. Soc.* **127**, 13496–13497.
9. Pelly, S. C., S. Govender, M. A. Fernandes, H. G. Schmalz and C. B. De Koning, C. B. (2007) Stereoselective syntheses of the 2-isopropenyl-2,3-dihydrobenzofuran nucleus: Potential chiral building blocks for the syntheses of tremetone, hydroxytremetone, and rotenone. *J. Org. Chem.* **72**, 2857–2864.
10. Lee, S. T., T. Z. Davis, D. R. Gardner, S. M. Colegate, D. Cook, B. T. Green, K. A. Meyerholtz, C. R. Wilson, B. L. Stegelmeier and T. J. Evans (2010) Tremetone and structurally related compounds in white snakeroot (*Ageratina altissima*): A plant associated with trembles and milk sickness. *J. Agric. Food Chem.* **58**, 8560–8565.
11. Davis, T. Z., S. T. Lee, M. G. Collett, B. L. Stegelmeier, B. T. Green, S. R. Buck and J. A. Pfister (2015) Toxicity of white snakeroot (*Ageratina altissima*) and chemical extracts of white snakeroot in goats. *J. Agric. Food Chem.* **63**, 2092–2097.
12. Panter, K. E. and L. F. James (1990) Natural plant toxicants in milk: A review. *J. Anim. Sci.* **68**, 892–904.
13. Bonner, W. A., J. I. De Graw, D. M. Bowen and V. R. Shah (1961) Toxic constituents of "white snakeroot". *Tetrahedron Lett.* **2**, 417–420.
14. Zhou, F., Y. Cheng, X. P. Liu, J. R. Chen and W. J. Xiao (2019) A visible light photoredox catalyzed carbon radical-mediated generation of *ortho*-quinone methides for 2,3-dihydrobenzofuran synthesis. *Chem. Commun.* **55**, 3117–3120.

15. Blum, T. R., Y. Zhu, S. A. Nordeen and T. P. Yoon (2014) Photocatalytic synthesis of dihydrobenzofurans by oxidative [3 + 2] cycloaddition of phenols. *Angew. Chem. Int. Ed.* **53**, 11056–11059.
16. Baptista, M. S., J. Cadet, A. Greer and A. H. Thomas (2021) Photosensitization reactions of biomolecules: definition, targets and mechanisms. *Photochem. Photobiol.* **97**, 1456–1483.
17. Baptista, M. S., J. Cadet, P. Di Mascio, A. A. Ghogare, A. Greer, M. R. Hamblin, C. Lorente, S. C. Nunez, M. S. Ribeiro, A. H. Thomas, M. Vignoni and T. M. Yoshimura (2017) Type I and type II photosensitized oxidation reactions: guidelines and mechanistic pathways. *Photochem. Photobiol.* **93**, 912–919.
18. Ghogare, A. A. and A. Greer (2016) Using singlet oxygen to synthesize natural products and drugs. *Chem. Rev.* **116**, 9994–10034.
19. Dethe, D. H. and B. D. Dherange (2015) Enantioselective total syntheses of (+)-hostmanin A, (−)-linderol A, (+)-methyllinderatin and structural reassignment of adunctin E. *J. Org. Chem.* **80**, 4526–4531.
20. DellaGreca, M., M. R. Iesce, L. Previtera, R. Purcaro, M. Rubino and A. Zarrelli (2008) Lignans by photo-oxidation of propenyl phenols. *Photochem. Photobiol. Sci.* **7**, 28–32.
21. Wang, Y., J. Wu and P. Xia (2006) Synthesis of 1,1-dimethyl-4-indanol derivatives. *Synth. Commun.* **36**, 2685–2698.
22. Durantini, A. M., L. E. Greene, R. Lincoln, S. R. Martínez and G. Cosa (2016) Reactive oxygen species mediated activation of a dormant singlet oxygen

photosensitizer: From autocatalytic singlet oxygen amplification to chemicontrolled photodynamic therapy. *J. Am. Chem. Soc.* **138**, 1215–1225.

23. Lattanzi, A., A. Senatore, A. Massa and A. Scettri (2003) Novel highly regioselective $VO(acac)_2$/TBHP mediated oxidation of *o*-alkenyl phenols to *o*-hydroxybenzyl ketones. *J. Org. Chem.* **68**, 3691–3694.
24. Stephenson, N. A. and A. T. Bell (2005) Quantitative analysis of hydrogen peroxide by ^{1}H NMR spectroscopy. *Anal. Bioanal. Chem.* **381**, 1289–1293.
25. Charisiadis, P., C. G. Tsiafoulis, V. Exarchou, A. G. Tzakos and I. P. Gerothanassis (2012) Rapid and direct low micromolar NMR method for the simultaneous detection of hydrogen peroxide and phenolics in plant extracts. *J. Agric. Food Chem.* **60**, 4508–4513.
26. Durantini, A. M. and A. Greer (2021) Interparticle delivery and detection of volatile singlet oxygen at air/solid interfaces. *Environ. Sci. Technol.* **55**, 3559–3567.
27. Malek, B., W. Fang, I. Abramova, N. Walalawela, A. A. Ghogare and A. Greer (2016) 'ene' reactions of singlet oxygen at the air-water interface. *J. Org. Chem.* **81**, 6395–6401.
28. Li, J., L. Wang, J. Li, Y. Shao, Z. Liu, G. Li, and E. U. Akkaya (2022) Taming of singlet oxygen: Towards artificial oxygen carriers based on 1,4-dialkylnaphthalenes. *Chem. Eur. J.* e202200506.
29. Wilkinson, F., W. P. Helman and A. B. Ross (1995) Rate constants for the decay and reactions of the lowest electronically excited singlet state of molecular oxygen in solution. An expanded and revised compilation. *J. Phys. Chem. Ref. Data* **24**, 663–677.

30. Manring, L. E. and C. S. Foote (1983) Chemistry of singlet oxygen. 44. Mechanism of photooxidation of 2,5-dimethylhexa-2,4-diene and 2-methyl-2-pentene. *J. Am. Chem. Soc.* **105**, 4710–4717.
31. Orfanopoulos, M., S. M. B. Grdina and L. M. Stephenson (1979) Site specificity in the singlet oxygen-trisubstituted olefin reaction. *J. Am. Chem. Soc.* **101**, 275–276.
32. Greer, A., G. Vassilikogiannakis, K. C. Lee, T. S. Koffas, K. Nahm and C. S. Foote (2000) Reaction of singlet oxygen with *trans*-4-Propenylanisole. Formation of [2 + 2] products with added acid. *J. Org. Chem.* **65**, 6876–6878.
33. Malek, B., W. Lu, P. P. Mohapatra, N. Walalawela, S. Jabeen, J. Liu and A. Greer (2022) Probing the Transition State-to-Intermediate Continuum: Mechanistic Distinction between a Dry versus Wet Perepoxide in the Singlet Oxygen "Ene" Reaction at the Air–Water Interface. *Langmuir* **38**, 6036–6048.
34. Brahmachari, G. and I. Karmakar (2020) Visible light-induced and singlet oxygen-mediated photochemical conversion of 4-hydroxy-α-benzopyrones to 2-hydroxy-3-oxo-2,3-dihydrobenzofuran-2-carboxamides/carboxylates using Rose Bengal as a photosensitizer. *J. Org. Chem.* **85**, 8851–8864.
35. Jabeen, S., M. Farag, B. Malek, R. Choudhury and A. Greer. (2020) A singlet oxygen priming mechanism: Disentangling of photooxidative and downstream dark effects. *J. Org. Chem.* **85**, 12505–12513.
36. Celaje, J. A., D. Zhang, A. M. Guerrero and M. Selke (2011) Chemistry of trans-resveratrol with singlet oxygen: [2 + 2] addition, [4 + 2] addition, and formation of the phytoalexin moracin M. *Org. Lett.* **13**, 4846–4849.

37. Carteau, D., P. Brunerie, B. Guillemat and D. M. Bassani (2007) Photochemistry in everyday life: The effect of spontaneous emulsification on the photochemistry of *trans*-anethole. *Photochem. Photobiol. Sci.* **6**, 423–430.
38. Helesbeux, J. J., O. Duval, C. Dartiguelongue, D. Séraphin, J. M. Oger and P. Richomme (2004) Synthesis of 2-hydroxy-3-methylbut-3-enyl substituted coumarins and xanthones as natural products. Application of the Schenck ene reaction of singlet oxygen with *ortho*-prenylphenol precursors. *Tetrahedron* **60**, 2293–2300.
39. Helesbeux, J. J., O. Duval, D. Guilet, D. Séraphin, D. Rondeau and P. Richomme (2003) Regioselectivity in the ene reaction of singlet oxygen with *ortho*-prenylphenol derivatives. *Tetrahedron* **59**, 5091–5104.
40. Helesbeux, J. J., D. Guilet, D. Séraphin, O. Duval, P. Richomme and J. Bruneton (2000) *Ortho*-prenylphenol photooxygenation as a straightforward access to *ortho*-(2-hydroxy-3-methylbut-3-enyl)phenols. *Tetrahedron Lett.* **41**, 4559–4562.
41. Griesbeck, A. G., M. Fiege, M. S. Gudipati and R. Wagner (1998) Photooxygenation of 2,4-dimethyl-1,3-pentadiene: Solvent dependence of the chemical (ene reaction and [4 + 2] cycloaddition) and physical quenching of singlet oxygen. *Eur. J. Org. Chem.* **1998**, 2833–2838.
42. Kitamura, N., K. Yamada, K. Ueno and S. Iwata (2006) Photodecomposition of phenol by silica-supported porphyrin derivative in polymer microchannel chips. *J. Photochem. Photobiol. A Chem.* **184**, 170–176.

FIGURE AND TABLE CAPTIONS

Figure 1. Synthesis of dihydrofuran (*R*)-**2** with the structure of tremetone (*R*)-**3** shown to the right.

Figure 2. Proposed mechanism in the sensitized photooxidation of prenyl phenol **4**, including solvent and DABCO additive effects.

Figure 3. Normalized $^1O_2$ luminescence decay curves monitored at 1270 nm with increasing concentration of prenyl phenol **4** in (A) C_6H_6 and (B) CH_3OH.

Figure 4. Plots of k_{obs} (s^{-1}) values as a function of the concentration of prenyl phenol **4** in (A) C_6H_6 and (B) CH_3OH.

Table 1. Effects of solvent and DABCO additive on the product ratios in the photooxidation of prenyl phenol **4**.

Table 2. Total quenching rate constant (k_T) measurements of $^1O_2$ with prenyl phenol **4**.

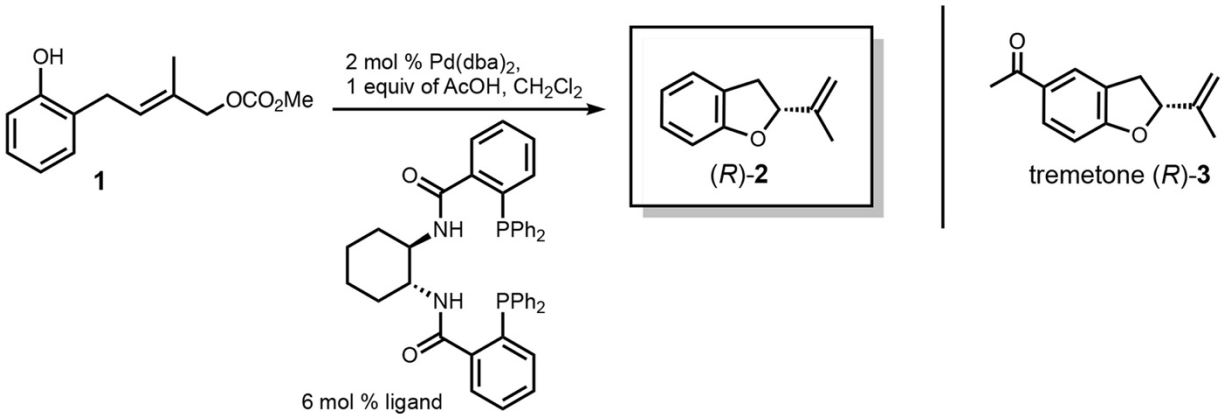

Figure 1. Synthesis of dihydrofuran (*R*)-**2** with the structure of tremetone (*R*)-**3** shown to the right.

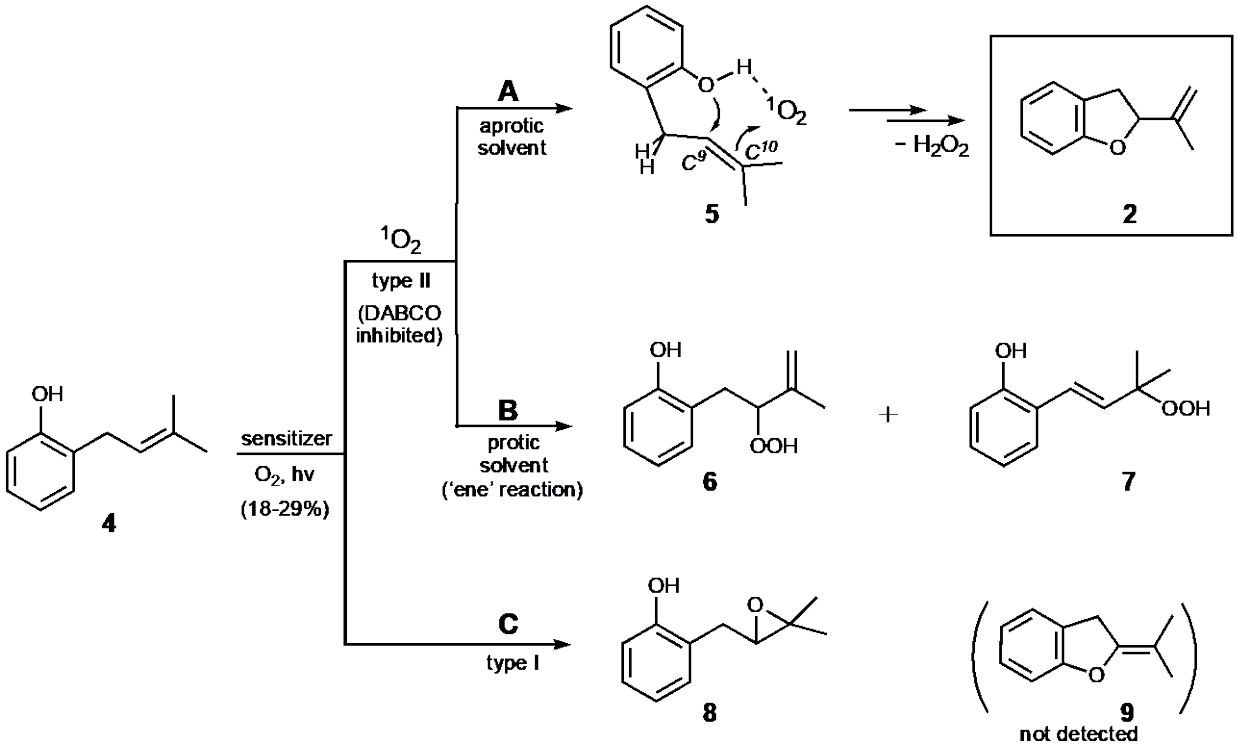

Figure 2. Proposed mechanism in the sensitized photooxidation of prenyl phenol **4**, including solvent and DABCO additive effects.

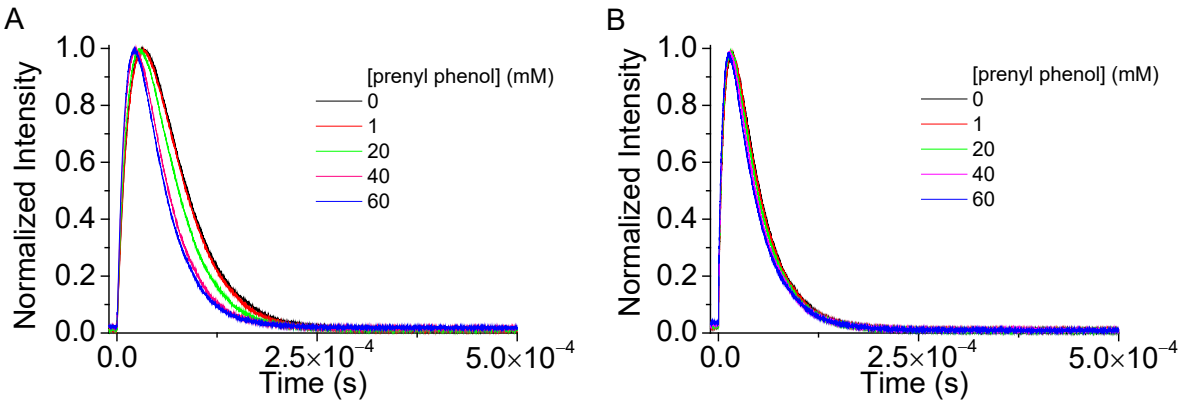

Figure 3. Normalized $^1O_2$ luminescence decay curves monitored at 1270 nm with increasing concentration of prenyl phenol **4** in (A) C_6H_6 and (B) CH_3OH.

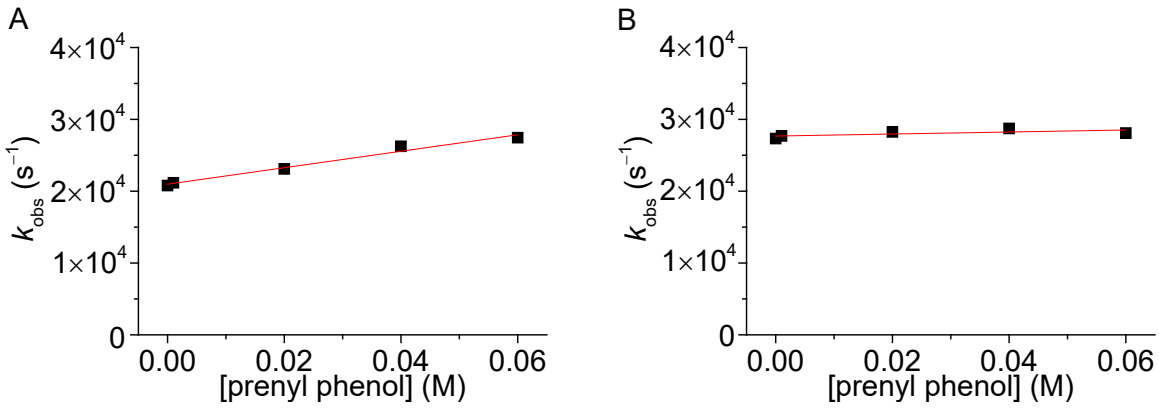

Figure 4. Plots of k_{obs} (s^{-1}) values as a function of the concentration of prenyl phenol **4** in (A) C_6H_6 and (B) CH_3OH.

Table 1. Effects of solvent and DABCO additive on the product ratios in the photooxidation of prenyl phenol **4**.

products	aprotic (C_6D_6)[a-c]	protic (CH_3OH)[b-d]
2	20.0 ± 4.0	5.1 ± 0.7
6	0.95 ± 0.07	3.0 ± 0.7
7	1.0 ± 0.03	3.5 ± 0.4
8	7.5 ± 2.2	6.7 ± 0.6

[a] Sensitizer TPP. [b] Addition of DABCO (2 or 10 mM) in the reactions led to an absence in the formation of **2**, **6**, and **7**, whereas **8** still formed and its yield unaffected. [c] Each value represents the mean of 4 separate experiments (mean ± SD). [d] Sensitizer $AlPcS_4$.

Table 2. Total quenching rate constant (k_T) measurements of $^1O_2$ with prenyl phenol **4**.[a]

solvent	k_T (M^{-1} s^{-1}) × 10^5
C_6H_6	1.29 ± 0.6
CH_3OH	0.12 ± 0.06

[a] Data represent the mean ± SD of 6 points at each concentration measured.